Fronts in the Atmosphere and Rotating Tank Laboratory

Elizabeth Maroon

April 22, 2009

Abstract

The thermal wind equation describes how a wind can be induced from a temperature or density gradient. In the Earth's atmosphere the stronger temperature gradient between the Earth's poles and equator creates the polar front and the upper level jets that circulate above it. We can create a lab analogue in the rotating tank with a sharp density difference. With the Margules Equation and velocities derived from particle tracks we are able to compare if our observed frontal angle is comparable to what Margules predicts. In the atmosphere we did a similar examination of both the polar front and synoptic-scale fronts to see how their winds and frontal angles compared.

1 Introduction and Theory

1.1 Overview

The Earth is warmed unevenly by radiation from the sun: the tropics receive more heat than the poles. Warm air takes up more space than does cool air, so at a given height, a column of air in the tropics with have a higher pressure than a column at the poles (see Figure 1). Pressure surfaces will slump down from equator to pole creating a temperature gradient. This temperature gradient is important as it is the origin of winds (like the jet) in the upper atmosphere of the Earth as exhibited by the thermal wind equation,

$$\frac{\partial \vec{u_g}}{\partial z} = -\frac{R}{fp}\hat{z} \times \nabla T \tag{1}$$

where $\vec{u}_g$ are the vector components of wind, R is the universal gas constant for dry air (a mix of nitrogen, oxygen, and other gases, excluding water vapor), f is the Coriolis parameter, p is pressure, and T is temperature (John Marshall and Illari 2003),(John Marshall and Illari 2003), (Illari and Marshall a).

Areas of stronger temperature gradient are known as fronts, and associated strong winds are called jets. In the atmosphere the juxtaposition between the cold polar air and the warm tropical air is known as the polar front. In the mid-latitudes where it occurs, we find an associated strong upper-level jet (Illari and Marshall (a)).

We can simulate fronts in the rotating tank laboratory by using a strong density gradient that has the same effect as a strong temperature gradient (see Figure 2). Jets

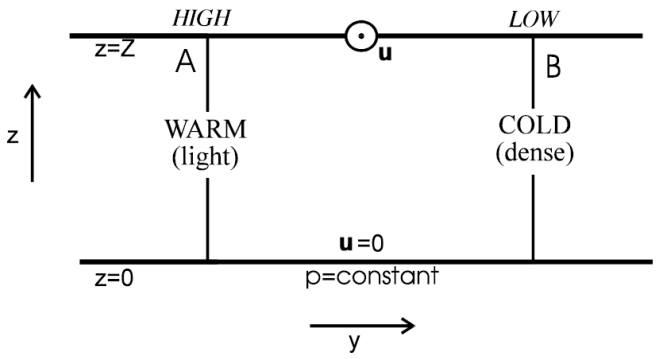

Figure 1: Air columns of differing temperatures. When comparing a warm air column and a cool air column, a major difference is found when looking on constant height surfaces. Warm air is more energetic and takes up more space than cool air; at a given height, the warm column will have a higher pressure than the cool column, because the more of the cool column's mass is below this surface. Pressure surfaces slant downward from the warm to the cool column, as they do from the equator to poles. This has important consequences when considering how temperature gradients effect upper-level winds. Image from Thermal Wind notes by John Marshall, Alan Plumb and Lodovica Illari at $http://www-paoc.mit.edu/12307/front/thermal\%20wind/thermal\_wind.pdf$. (John Marshall and Illari 2003)

can be observed at the surface and examined using the particle tracker. We can also measure the angle that the fronts make in the laboratory and compare it theoretical values.

1.2 Theoretical Importance

The thermal wind describes the relation between temperature gradients and winds; it is a result of the geostrophic balance and hydrostatic balance (when the Rossby number is small). The geostrophic wind, $\vec{u}_g$, is described by

$$\vec{u}_g = \frac{1}{\rho f}\hat{z} \times \nabla p \tag{2}$$

where rho is the density of the air, and $\hat{z}$ is the local up. When we take the partial of Equation 2 with respect to z and then substitute in the hydrostatic balance,

$$\frac{\partial p}{\partial z} = -\rho g \tag{3}$$

(where g is the gravitational constant 9.81 m/s^2 for the Earth's surface) we find the components in constant height coordinates as

$$\frac{\partial u_g}{\partial z} = \frac{g}{f\rho}\frac{\partial \rho}{\partial y} \tag{4}$$

and

$$\frac{\partial v_g}{\partial z} = -\frac{g}{f\rho}\frac{\partial \rho}{\partial x}. \tag{5}$$

The hydrostatic balance is appropriate as the vertical motions are relatively small

Figure 2: Setting up the rotating tank to create a front. By placing dense fluid (high salinity water) in the center of the rotating tank, we can create a dense cone surrounded by less dense water. This creates a density gradient capable of creating currents observable at the surface. These currents are analogous to jets high in the troposphere. Image from the Project 2 explanation by John Marshall and Lodovica Illari at $http://www-paoc.mit.edu/12307/front/project2.pdf$. (Illari and Marshall a)

(assuming little convection).

Once we add the Ideal Gas Law (because the atmosphere can be approximated well as an ideal gas)

$$p = \rho RT, \tag{6}$$

with some rearranging, we find the thermal wind equations in constant height coordinates as

$$\frac{\partial \vec{u_g}}{\partial z} = -\frac{R}{fp}\hat{z} \times \nabla T \tag{7}$$

It is important to note that the thermal wind equation will differ depending on whether or not the fluid is compressible. Water, being incompressible, is subject to a density anomaly as

$$\rho = \rho_0 + \delta\rho \tag{8}$$

where ρ_0 is the reference density, $\delta\rho$ is the variation in density and $\frac{\delta\rho}{\rho_0} << 1$. In water, density and temperature are linearly related by $\rho = \rho_0(1 - \alpha(T - T_0))$ where T_0 is a reference temperature and α is an expansion coefficient for the fluid. This would transform the thermal wind equation in height coordinates to

$$\frac{\partial \vec{u_g}}{\partial z} = -\frac{\alpha g}{f}\hat{z} \times \nabla T. \tag{9}$$

This works for our incompressible tank experiments, but in the compressible atmosphere it is more convenient to work in pressure coordinates. If we start with the geostrophic relation (Equation 2) and take its partial derivative with respect to pres-

sure, and then substitute with the hydrostatic relation and ideal gas law, we will find

$$\frac{\partial u}{\partial p} = \frac{R}{fp}\left(\frac{\partial T}{\partial y}\right)_p ; \frac{\partial v}{\partial p} = -\frac{R}{fp}\left(\frac{\partial T}{\partial x}\right)_p ; \tag{10}$$

In these experiments it will be useful to have a discrete form of the thermal wind equation, known as the Margules Equation. The Margules Equation gives us a clear way to measure the slope of the front and the angle at which warm air aloft and cold air below meet. For the tank experiments where we will be measuring a discrete density difference across the front it is easiest to show the Margules Equation as

$$v_2 - v_1 = \frac{g' tan(\gamma)}{f}, \tag{11}$$

where $v_{1,2}$ are velocities parallel to the front, with one above and one below. g' is the reduced gravity which is equal to $g\frac{\rho_2 - \rho_1}{\rho_2}$. The two densities are the densities found with each velocity. Without direct access to density, we find it easier to put the Margules Equation in terms of temperature through use of the ideal gas law

$$tan(\gamma) = \frac{f(v_2 - v_1)}{g(T_1 - T_2)/T}. \tag{12}$$

This version of the Margules Equation is useful for calculating the slope of fronts in the atmosphere where temperature is easily measurable with radiosondes. It is very useful in determining if our observations match what theory expects them to be (John Marshall and Illari 2003),(Illari and Marshall b), (Illari and Marshall a).

2 Fronts in the Rotating Tank

2.1 Procedure

An analogue for the polar front and jets can be created in a tabletop rotating tank. However, creating a long-lasting temperature gradient (as seen between the poles and equator) would be difficult given the level of mixing that occurs. Instead, temperature is held constant and we vary the density of the fluids. The density of water is increased by adding a great deal of salt and increasing the $\delta\rho$.

We place a can in the middle of the tank, and seal it from the outer low density water with a non-polar substance (such as Vasoline) so that no dense water will escape until ready. The rotating tank is set to a speed and allowed to reach solid body rotation. Upon reaching a steady state, the inner can is lifted straight up, releasing the high density water into the low density water. It creates a cone of dense water, and the gradient across the front creates surface currents that are observed by particle-tracking software in the frame of the spinning tank.

Besides measuring these currents, we can directly measure the density inside and outside of the cone. We can also visually observe and photograph the angle of the front. With these two pieces of data, we can compute the expected velocities and compare them to those that we observed.

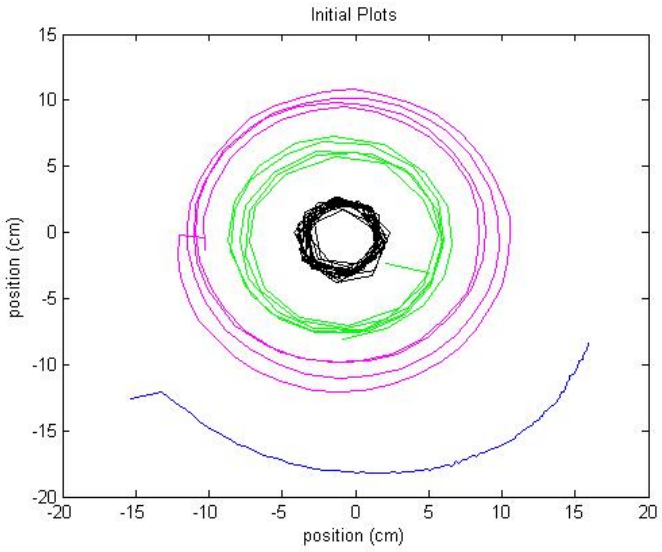

Figure 3: Plot of particle tracks for the 10 rpm trial. Our first trial at 10 rpm showed excellent particle tracks for which we were able to calculate velocities in the currents (j̈ets ̈). Each track rotated about a common center. The velocities decreased as the particles were further removed from the front.

2.2 Results

We had two trials for this experiment; during the first our rotation speed was 10 rpm, and during the second, 15 rpm. The first data set had steady circular particle tracks that would be easy to analyze (see Figure 3). The second data set never reached a steady state; unlike the first experiment where the dense cone did not move about the tank, the second experiment's cone moved through the tank. Particles became stuck to the tanks sides and bottom, and did not make clean rotational paths that would be easily analyzable (see Figure 4).

We measured the density difference between the light and dense fluids for both cases. In experiment 1, the light fluid was 1.002 g/mL and the dense fluid was 1.038 g/mL. In the second experiment, the light fluid's density was 1.037 g/mL, and the dense fluid's density was literally off the charts. We chose the greatest value possible, 1.075 g/mL, but this increased even more uncertainty into experiment 2.

For Experiment 1, we photographed the frontal surface to determine the angle of the front (see Figure 5).

Once we had all three pieces of information, we were ready to start analyzing.

2.3 Analysis and Discussion

For the tank experiment at 10 rpm, we change the particle tracks into a polar coordinate system and find their azimuthal velocities, v_θ (which happen to be our thermal wind currents) by

$$v_\theta = r\frac{\partial\theta}{\partial t} \approx r\frac{\Delta\theta}{\Delta t}. \tag{13}$$

We can easily measure the change in angle ($\Delta\theta$) over each incremental change in time (Δt). When we analyze each of the 4 tracks, we find that the tracks nearest the center

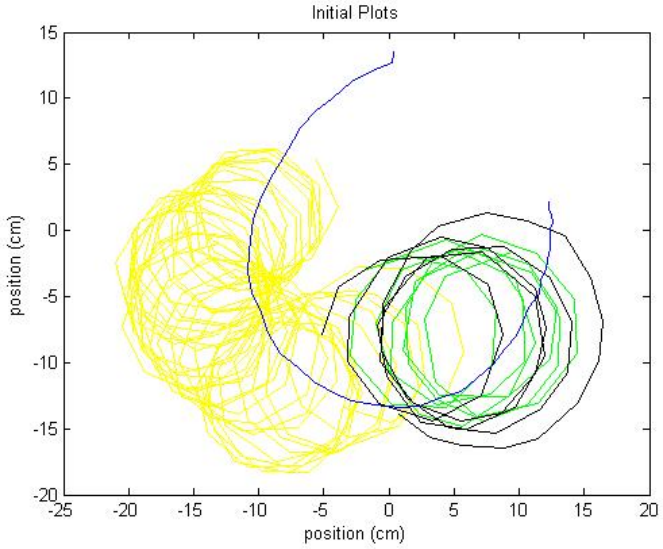

Figure 4: Plot of particle tracks for the 15 rpm trial. Our second trial at a higher rotation speed had a dense cone that moved all around the tank and never reached steady state. Note that most tracks included had circular paths. There were initially more paths in this view, paths of submerged and stationary particles that made this image more confusing. Although we could have taken a single loop from these paths and analyzed them, the cone's velocity component would still be buried in it. Our first data set had no issues, and we worked mostly with those tracks.

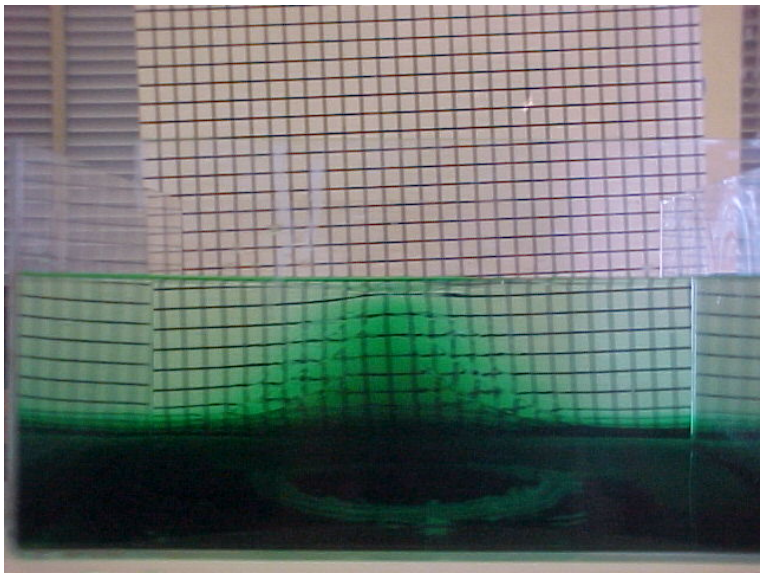

Figure 5: Photo of the frontal angle for Experiment 1. The dense, dyed fluid (green) forms a cone under the lighter, clear fluid. The analogy to the Earth's atmosphere is that the green cone is the cold pole, and the clear fluid is the tropical air. Although it is not very visible in this image, above the center of the cone there was a slight dip in the surface, indicating that this is the area of low pressure.

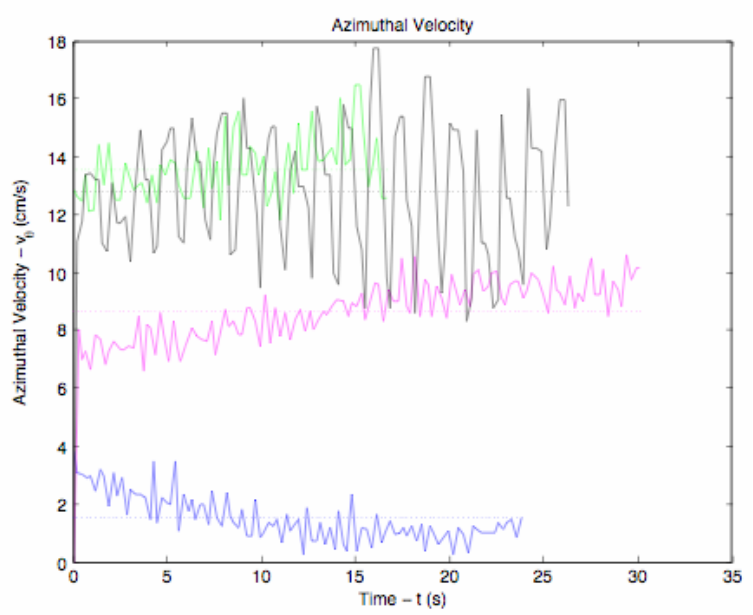

Figure 6: Azimuthal velocity as a function of time. For our 10 rpm experiment, we found that the tracks closest to the center had the greatest velocities after comparing to Figure 3. The colors in this figure correlate to those in Figure 3. Fluctuations are likely from not pinpointing the exact center of rotation.

(and closest to the temperature gradient) have the greatest velocities as seen in Figure 6.

Over the center of rotation, the free surface dipped down, as expected over a cold/more dense column. Here is where there is a low pressure and since the surface pressure is set, seeing it have a lower height is a rewarding verification to the theory. The black and green tracks on Figures 3 and 6 are on the slope leading to this depression. The thermal winds were less when they were further from the major density jump.

The next step is to compare the observed frontal slope to the slope expected by the Margules Equation. After photoshopping our image and using pixels to calculate the slope and angle (see Figure 7), we found that frontal angle to be 40°.

Using the Margules Equation with the maximum velocity (the black track) and assuming that the velocity far from this point is approximately 0, we esimtated an average frontal slope of 39°. The unusual correlations between the Margules Equation and our observations of the frontal surface is helped by our great particle tracks. However, this great correlation is also a product of luck, given our estimations in the frontal surface and in 1-sample density observations.

3 Fronts in the Atmosphere

3.1 The Polar Front

The tank experiments are meant to be an analogue for the polar front of Earth's mid-latitudes. Here is where the cold polar air slips underneath the warm tropical air. We used both current and climatological data to examine the phenomenon of temperature

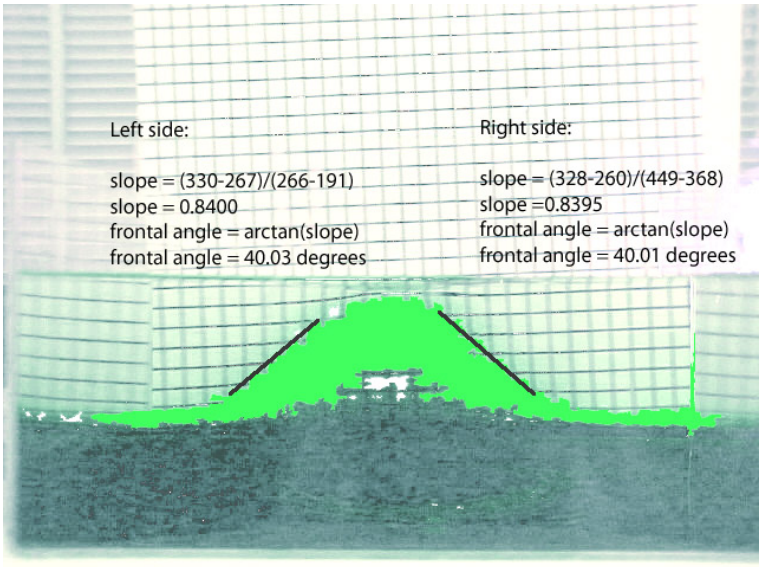

Figure 7: Calculation of the front by photoshopping and pixel counting. After using photoshop to clear up the boundary between the two densities, we found the average slope for the middle range of the front. We found the average angle for this main portion of the front to be 40°. Had photoshop been even more accomodating, we could have found the slopes for the entire front, instead of just an average.

gradients and jets.

On March 12, 2009, we examined the current temperature state of the northern hemisphere at 500 mb (see Figure 8). After visually examining the current data, the 150 longitude line (over the Pacific ocean near Siberia) was chosen for a cross-section (see Figure **??**) given its larger temperature gradient. In the cross-section we see a few interesting features.

In climatological data, we also see a polar front when we examine pressure surfaces around 500mb in the middle troposphere during February. After gathering data sets from NOAA we run the data through a program that shows us the zonal velocities and the temperature gradients. Figure 10 shows the greatest magnitude of of wind shear around 40 latitude, which is also where we would expect to find the polar front in February.

However, the plot of the residuals (the differences) when comparing the wind shear from the temperature gradient side (thermal wind equation) with wind shear from wind observations, is working well (see Figure 11), and here we again see that these residuals (the actual wind shears minus the observed wind shears) are close to zero. This indicates that the two agree fairly well. We do see that the least agreement is see around 30 degrees north, possibly because the calculated wind shears are expecing a stronger front at a lower altitude than is actually observed.

3.2 Synoptic Scale Fronts

Also frequent in the mid-latitudes are synoptic-scale fronts. Depending on the temperature of the air mass moving the front, these fronts are designated as warm or cold fronts. Often in the cyclonic circulation of low pressure systems, we find warm, moist air being brought northward (warm front), and cold, dry being brough southward (cold

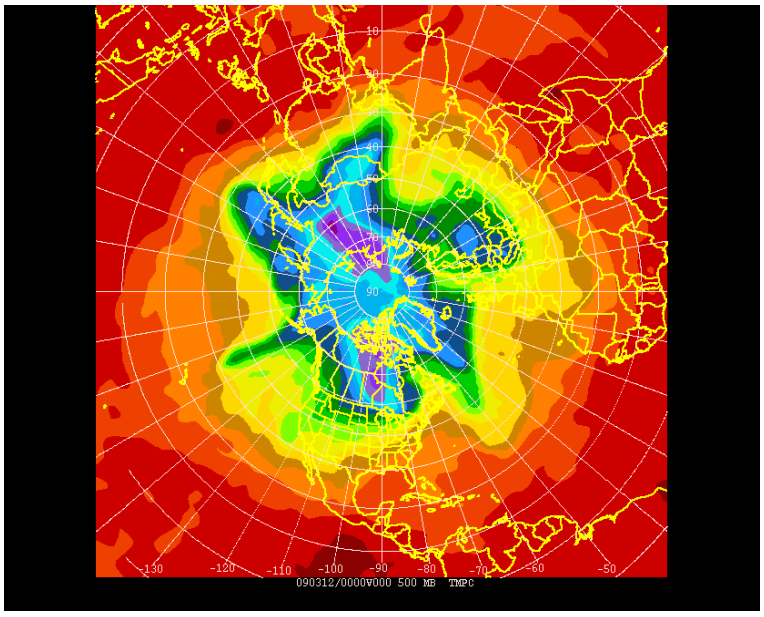

Figure 8: 500 mb temperature of the northen hemisphere on March 12, 2009. The polar front occurs at the greatest gradiation of color, where the cold polar air is meeting the warm tropical air. The 150 mb longitude line over eastern Siberia and the Pacific ocean was chosen for a cross section (to examine the polar front) as it has one of the greatest and sharpest temperature gradients.

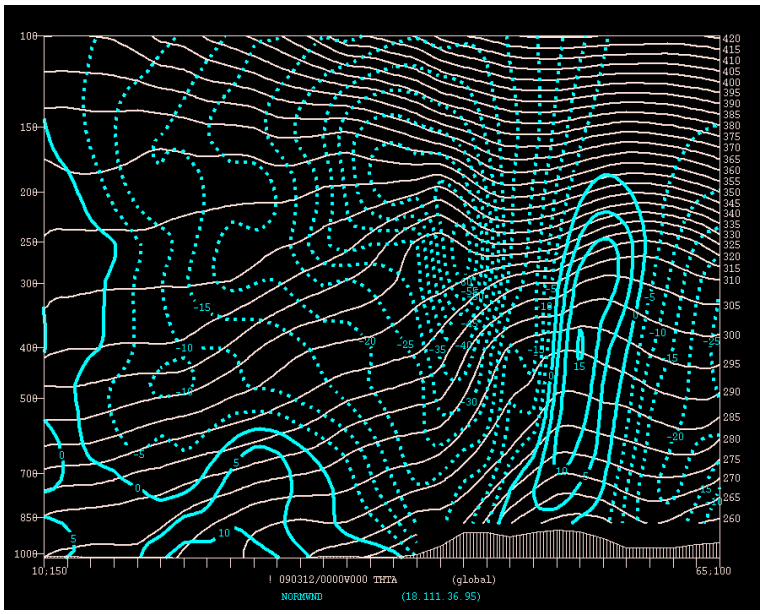

Figure 9: Cross section at 150 longitude on March 12, 2009. Notice the cyclonic circulation with the expected jet at 300 mb coming out of the page and the other strong wind at 450 mb moving into the page. The upper-level jet occurs above the maximum temperature gradient in the mid-latitudes, as expected by the thermal wind equation.

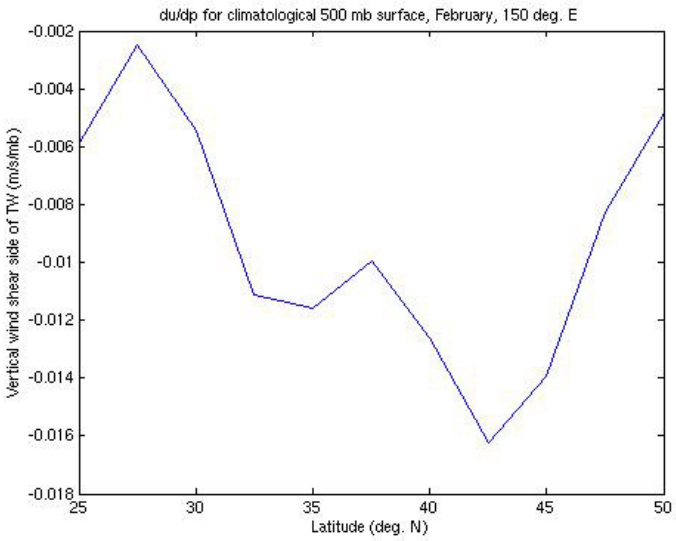

Figure 10: Wind Shear versus latitude of the February 500 mb climatological surface. Notice that the greatest magnitude of wind shear occurs at 40-45 degrees latitude, above where the polar front would be found.

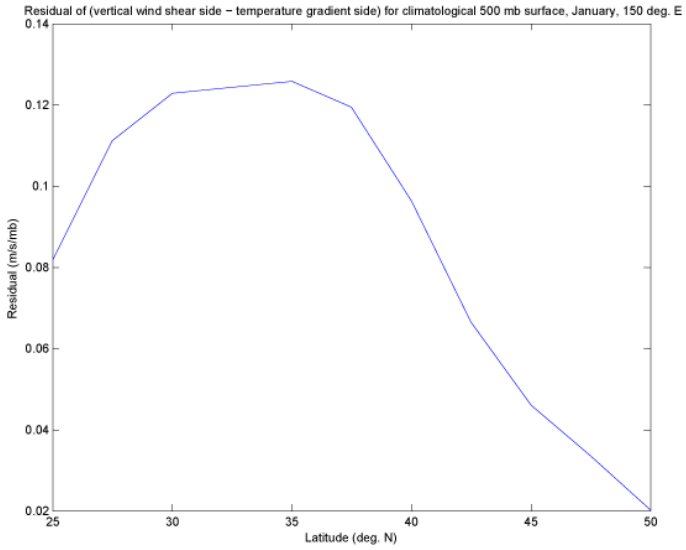

Figure 11: Climatological vertical wind shear residuals. Here we see the residuals from the two methods for collecting vertical wind shear, from the temperature gradient (through the thermal wind equation) and from wind observations for the climatological 500 mb surface in February over 150 degrees East. Notice that these values are fairly low, much less than one, indicating the good fit between the temperature and wind observation with the theory.

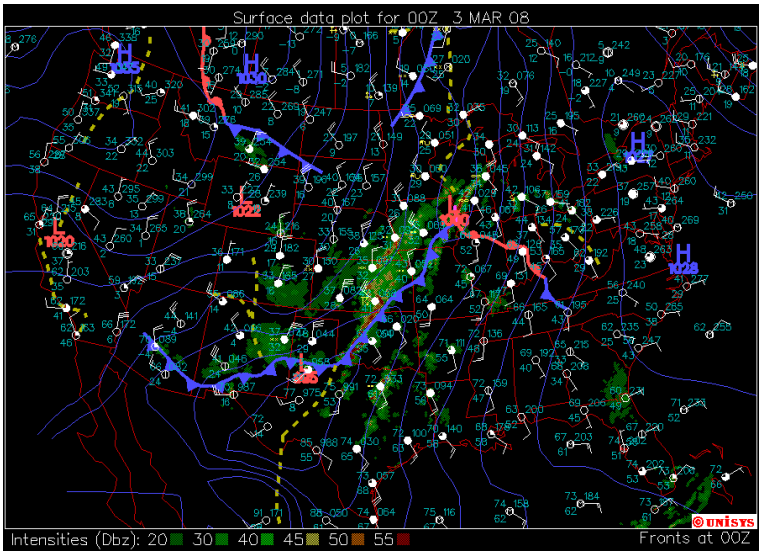

Figure 12: Synoptic Condition of the United States for March 3, 2008 at 00 UTC. Notice the low pressure centered on Iowa and the long, strong cold front that stretches from there to Arizona. Behind this cold front (where warm air has been forced up) we see lots of precipitation and severe weather. It was on this day that Oklahoma experienced a few tornadoes. There is a warm front that stretches from Iowa through Indiana.

front). This often creates an area of warm air between the fronts called the warm sector. Either way, when warmer moist air rises above colder air, water will condense and precipitate.

We chose a case study from March 2-4 in 2008 that had a strong low pressure system with associated strong winds, hail and tornadic activity (NWS SPC, 2008)Center (March 2008). We chose a time in the storm when the temperature gradient acoss both fronts was strongest on March 3rd at 00 UTC. Figure 12 displays the current synoptic conditions and Figure 13 shows the strong temperature gradients. In Figure 13, we examined our warm front to the north of here on a cross-section from the northeastern tip of Illinois to approximately 200 miles north of upstate New York in Canada. The cross-section for the cold front stretches from north-central Texas to northeastern Colorado. We examined these cross-sections to see the angle of the front and compare it to the one expected by the angle predicted by the Margules Equation.

We took cross-sections of the warm and cold fronts (see Figures 15 and 16) for March 3rd using the Synoptic Lab's cross-section website, and found the angle of the fronts by using the hydrostatic balance to estimate the Δz of the front, and the Δx with the horizontal length that the front stretched. We then used the Margules Equation (as in Equation 12) with the wind speeds and temperatures provided on the cross-sections. We also showed in Figure 14 how potential temperature shows a colder dome to the cold side of the warm front. (The effect is the same for the cold front, and further figures for the cold front would only be repetitive.) Constant potential temperature shows the contours that are adiabatic (no heat lost) when changing pressure and temperature. If an air parcel is brought down from a lower pressure along a constant potential temperature line, no heat would be lost from the parcel, but its temperature would increase because of the increasing pressure. This allows us to see air that is overall colder in a dome to the cold side of our fronts, much in a pattern like we had a cold

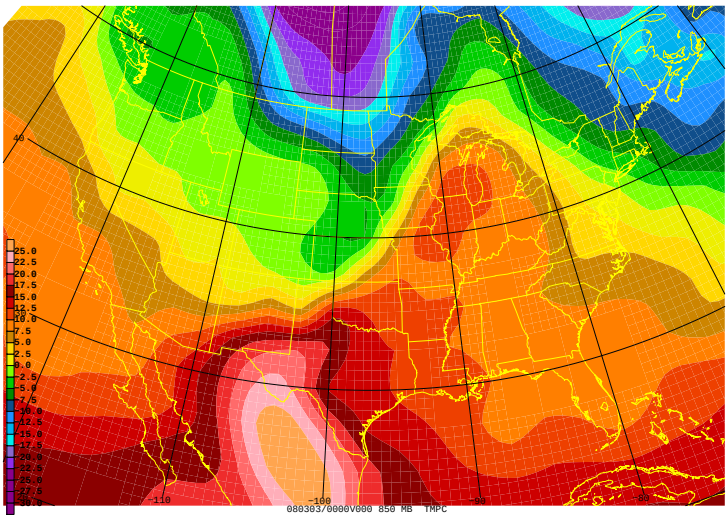

Figure 13: Temperature plot of the United States for March 3, 2008 at 00 UTC. Here we can clearly see the warm sector over Missouri, Illinois and Michigan.

high salinity dome in the tank experiment.

3.3 Atmospheric Analysis and Discussion

If we had estimations in our tank data, then our atmospheric data had just as many approximations when attempting to find the slope as observed and by the Margules formula. We found that there was correlation between the climatological data when looking at the temperature gradients on specific pressure surfaces.

For the synoptic plots we calculated the observed slope by $tan(\gamma) = \frac{\Delta z}{\Delta x}$ where Δz was determined using the hydrostatic relation with the ideal gas law $\Delta z = \frac{R\overline{T}}{g} ln(\frac{p_{bottom}}{p_{top}})$. The average temperature was estimated as the average temperature across the front.

What kind of values are we expecting? We can use a non-dimensional number to determine the expected slopes in our system using the Rossby number and the Rossby radius of deformation which is equal to $\sqrt{g'H}/2\Omega L$. For the warm and cold fronts described below this will give us values of around $1/100$.

For the warm front, we used Figure 15 to find $p_{bottom} = 875, p_{top} = 600, R = 287, and \overline{T} = 273K$ to determine that $\Delta z = 2543m$. $\Delta x = 299km$ which means our observed frontal slope is $0.49°$. When we use temperature and velocity conditions picked from the same figure over the front ($\phi = 45; f = 2\Omega sin(\phi); T_{front} = 270K; T_1 = 266K; v_1 = -10; T_2 = 277K; v_2 = 0$), then the Margules formula predicts an angle of $1.44°$. When we do the same analysis on the cold front, our observations give us a frontal angle of $0.74°$ and the Margules Equation gives us an angle of $2.25°$. For both the observations and the Margules-derived angle, we see that the cold front has a slightly steeper angle (and with it stronger wind shear). However the difference between the observed and Margules frontal angles in both cases is a little disconcerting. There was a lot of estimations in these calculations (particularly given the resolution of the images).

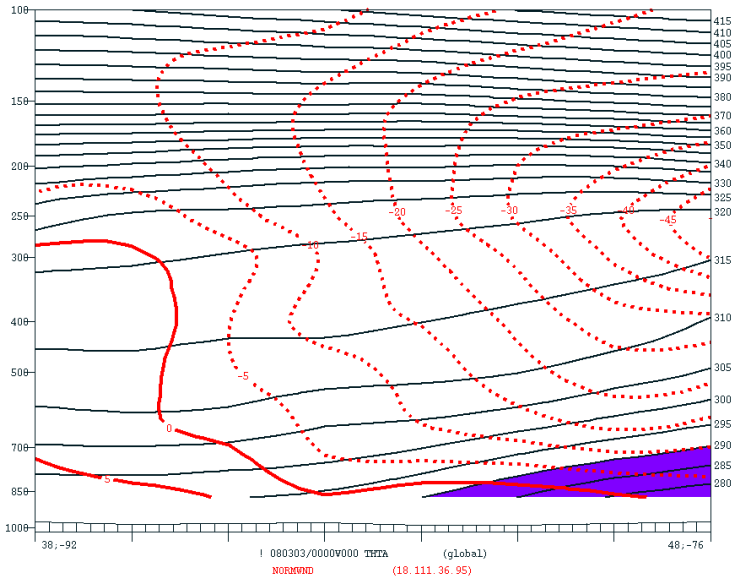

Figure 14: Cross section of potential temperature on the warm front across the upper Great Lake state on March 3 at 00 UTC. Note the blue cold air dome to the right of the warm front. The frontal surface is very clear along the contours of potential temperature.

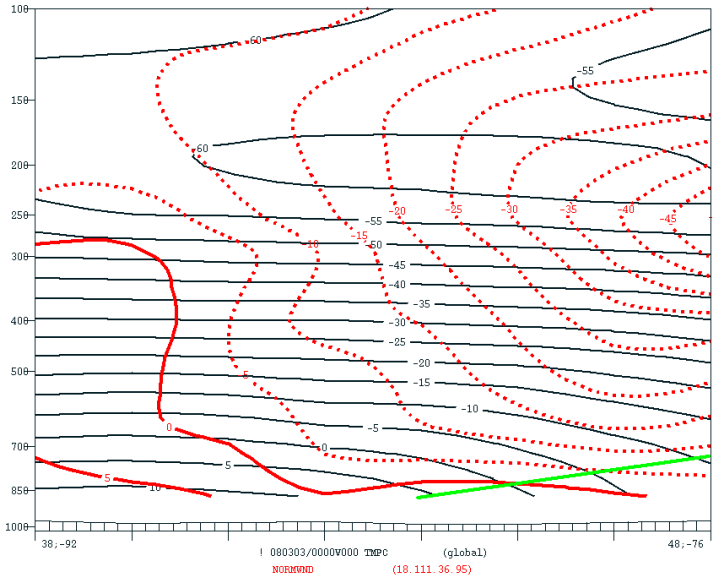

Figure 15: Cross section of temperature on the warm front across the upper Great Lakes states on March 3 at 00 UTC. The wind shear across the warm front (the red contours) is present, but not as strong as in the warm front. The green contour denotes the approximate slope of the frontal surface. The greater horizontal distance covered by the front also contributes the shallower frontal angle.

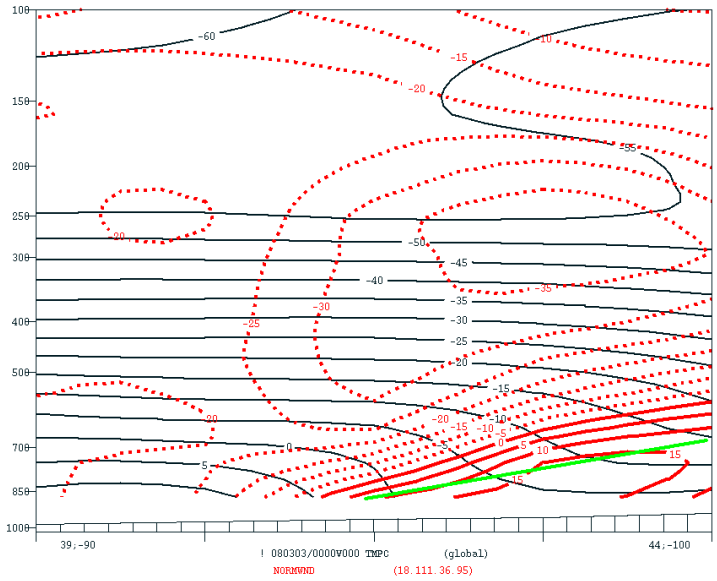

Figure 16: Cross section of the cold front across the plain states on March 3 at 00 UTC. Winds are denoted by the red contours and the approximate frontal surface by the green. We have calculated a steeper frontal angle than in the warm front which comes with a much greater wind shear (of about 30 knots) across the front.

Is it valid to try to calculate the frontal slope at warm and cold fronts? Some of the assumptions that were made were small Rossby number and hydrostatic balance. But at a synoptic-scale front, geostrophic balance may not be the best assumption; and if there is convection occuring at the front as cold air slides under warm air, then there is a vertical velocity, making hydrostatic balance invalid. The Margules Formula also assumes that the front is a discontinuity with a sharp transistion from cold to warm, which is also not necessarily valid. Smaller-scale processes at synoptic fronts make the Margules Equation less valid than in the tank experiment. This could account for some of the discrepancies between the two calculated angles at the synoptic fronts.

4 Connections and Conclusions

One of the main differences between the frontal slopes in the tank experiment and in the atmosphere is the scales. Given the height of the tank and the relatively high rotation rate (the Earth rotates at a much slower rotation), the cold cone had a steeper angle. The relatively thin-height of the troposphere (which is on the order of 10 km next to the Earth's 6370 km) shows when the Δx is compared with the Δz. The height of fronts in the atmosphere is 3 orders of magnitude less than the horizontal distance that they cover. Another difference is the medium's properties; air in the atmosphere is compressible, while water in the tank is incompressible.

However, there are more fundamental similarities than dissimilarities between the tank experiment and the atmospheric analyses. Both have a low pressure found over the cone of more dense material in the center of the tank, or over the cold pole. The jets in both move cyclonically (counterclockwise in the northern hemisphere), and

are strongest over the area of greatest temperature/density gradient. Both are stable situations with heavier fluid under light fluid and both try to reach an equilibrium. As the tank has no new salt input, it will eventually reach an equilibrium with the less dense fluid, but the Earth is continually heated by the sun, keeping the disequilibrium in motion.

This study of fronts showed the relations between temperature, density, pressure, and winds when we consider cases that are geostrophic, hydrostatic, and ideal. In our tank experiment, we found that the thermal wind equation and the Margules Equation adequately describe the situations in both the rotating tank and at the polar fronts. Stronger winds are found circulating over areas of strong temperature and density gradients.

5 Future Work

It would be useful to examine other rotational speeds for the tank experiment; only one of our speeds produced decent data. It would be interesting to compare the heights for the central low at various (faster) speeds. For future work, it would also be useful to find the instantaneous slope along the tank experiment's front. This would require more accurate particle tracks and a way to find many slopes from the photo of the cone. Some photo-editting/analyzing software that could identify the pixels at the boundary and calculate the slope between them would be useful.

References

NWS Storm Precition Center. Spc storm reports, march 3, 2008, March 2008. URL http://www.spc.noaa.gov/climo/reports/080303$_r pts.html$.

Lodovica Illari and John Marshall. *Project 2: Fronts*. a.

Lodovica Illari and John Marshall. Weather in a tank: Fronts: Atmosphere - the polar front, b. URL http://www-paoc.mit.edu/labguide/fronts$_p olar.html$.

Alan Plumb John Marshall and Lodovica Illari. *Thermal Wind*. 2003. URL http://www-paoc.mit.edu/12307/front/thermal%20wind/thermal_wind.pdf.